

## AUTORADIOGRAPHIC AND HYDROTHERMAL PROBES OF INTERFACIAL CHEMISTRY IN OIL SHALE AND COAL

David S. Ross  
SRI International  
Menlo Park, CA 94025

Keywords: hydrous pyrolysis, autoradiography, maturation

### INTRODUCTION

The chemistry leading to the formation of petroleum hydrocarbons is an area of considerable interest, and major progress in our understanding has evolved in widely ranging studies over the past 25-30 years. The advances are due in large part to a broadening interest in the problem, encompassing large portions of the geochemistry, coal chemistry, and chemical kinetics communities, and to the development and application of new and sophisticated instrumentation.

However despite these advances, it is clear that there are still sizeable gaps in our perceptions of the processes, extending down to a very fundamental level. Thus for example, while the formation of petroleum is normally thought to be a geologically lengthy process involving the diagenetic breakdown and maturation of accumulated organic matter, it has been recently shown that petroleum hydrocarbons can be formed in much shorter periods of time in sedimented, submarine rift basins at 280°-350°C (Simoneit, 1985; Simoneit, et al., 1987). The products include an *n*-alkane distribution typical of petroleum, and highly condensed polynuclear aromatic hydrocarbons (PAHs) including phenanthrene, pyrene, benzpyrenes and coronene. The alkane origins are unclear, as are those of the PAHs, which are commonly observed as products of hydrocarbon pyrolysis only at temperatures above 550°C, while coronene itself is not generated at temperatures below 650°C (Commins, 1969). These temperatures are obviously far greater than those in the vent region, and the observations reflect the operation of largely unexplored but significant chemical processes.

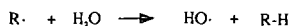
One of the tools widely used in maturation studies is hydrous pyrolysis, or the heating of immature sediment in liquid water at pyrolytic conditions at 290-360°C (Lewan et al., 1979; 1981). (The critical temperature of water is 374°C.) The process is thought to accelerate maturation so that hydrocarbon development can be examined in a laboratory setting, although the claim that the procedure exactly mimics the natural process has been questioned (Monthieux et al., 1985; Tannenbaum and Kaplan, 1985; Comet et al., 1986).

Whatever the case, the chemistry of very hot water at the organic-mineral boundary is central to question of hydrocarbon production. Specific key issues are the nature of bonding at the interface, and effects of water in the hydrothermal regime on the chemistry. The discussion here offers some thoughts on those questions, drawing upon both our interpretation of hydrous pyrolysis data by Hoering (1984), and our work on organic/mineral interfacial interactions.

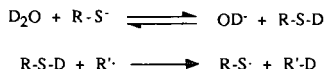
### BACKGROUND

In studies of maturation it has been shown that the presence of liquid water increases the pyrolysate yield (Comet et al., 1986) and minimizes or eliminates the high olefin yields seen in dry pyrolysis (Hoering, 1984). It is often suggested that the key role of water in

hydrous pyrolysis is to cap pyrolytically formed organic free radicals (Monthioux et al., 1985; Hoering, 1984; Comet et al., 1986).



However this reaction is endothermic by 25-30 kcal/mol, and cannot be significant at hydrous pyrolysis temperatures. We have recently pointed out that if free radical chemistry is significant in hydrous pyrolysis, a more likely route is rapid, initial ionic deuterium-protium exchange between  $D_2O$  and a phenol, a thiol, or  $H_2S$ , followed by deuterium atom transfer to organic free radical sites (Ross, 1992).



On the other hand there is no compelling evidence at present supporting any specific mechanistic route.

Nonetheless some sense of the sequence for hydrocarbon production can be developed with attention to the hydrous pyrolysis work by Hoering (1984). He reported on the treatment of finely divided samples of Messel shale with  $D_2O$  at 330°C/3 days, under which conditions about 8% of the organic carbon was recovered as a mixture resembling petroleum hydrocarbons. The recovered products included a series of *n*-alkanes over the range  $C_{14}$ - $C_{30}$ , with each alkane itself comprised of a broad distribution of isotope isomers containing 0 to more than 14 deuterium atoms. The D-isomer distributions were all very similar, with the maxima spanning  $D_3$ - $D_6$  for the various alkanes, and with no apparent trend. Preexisting alkanes and olefins were ruled out as the source of the products by using source rock that had been previously extracted. The possibility that trapped alkanes surviving prior extraction were sources was eliminated in control experiments in which the source material was spiked with *n*-octadecane, which which then recovered after treatment with a considerably lower deuterium content than had been noted for the kerogen-derived material.

A particularly meaningful result was from work in which the starting shale was spiked with the olefin *n*-octadecene. Fully 60% of the olefin was recovered as the corresponding *n*-alkane, a result demonstrating the significant reduction potential available at hydrous pyrolysis conditions. Indeed, hydrogen is a common gaseous product in hydrous pyrolysis experiments (Lewan et al., 1979; 1981). The recovered alkane in this case contained deuterium, although the distribution was different from that found in the kerogen-derived alkanes. These results are discussed more fully below.

## RESULTS AND DISCUSSION

### Hydrous Pyrolysis and Deuterium Distribution

In considering Hoering's results, we seek to reconcile the data with a simple reaction model.\* The development here is primarily qualitative, and our goal is the simple compari-

\* A preliminary version of this work has recently appeared (Ross, 1992).

son of calculated and observed isotope isomer distributions. Detailed, quantitative reaction kinetics will be considered in a later development.

The basis of the process is the output from an integration routine based on the Gear algorithm (Moore and Pearson, 1981) and operated on a VAX 11/750 computer. The operation numerically simulates the sequential exchange in (1), presuming identical



rate constants for each step. (The kinetic isotope effects at these temperatures should be insignificant.) The output is a series of D-isomer profiles, with the major isomer moving to increasing substitution with time.

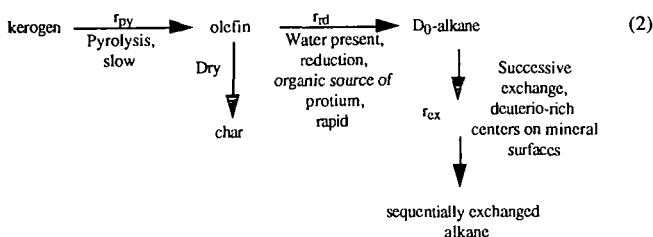
The deuterium contents in the alkanes recovered by Hoering in the alkane-added, the olefin-added, and the straightforward hydrous pyrolysis experiments are shown in Table 1. The table shows first that while the isotope substitution in the alkane-added experiment is small, there is nonetheless almost 30% exchange. Thus the *n*-alkane is not unreactive toward exchange in the system. In addition, in the face of a large excess of D<sub>2</sub>O, 9% and 4-6% of the olefin- and kerogen-derived alkane are D<sub>0</sub> respectively. These values are not insignificant and suggest that reduction of olefin from a strictly protio source precedes exchange, which then operates on the D<sub>0</sub> alkane.

Next, the D/H ratios show that despite their similar %-D values, the kerogen-derived alkane has experienced far more exchange than has the alkane recovered from the olefin-added study. This difference is displayed in Figure 1a which shows the isomer data for the kerogen-derived *n*-heptadecane, and in 1b which presents the distribution for the *n*-octadecane from added *n*-octadecene. In the former the distribution peaks at D<sub>3</sub> and extends to isomers beyond D<sub>14</sub>. In contrast the 1b peaks at D<sub>2</sub>, and no D-isomer is reported beyond D<sub>10</sub>.

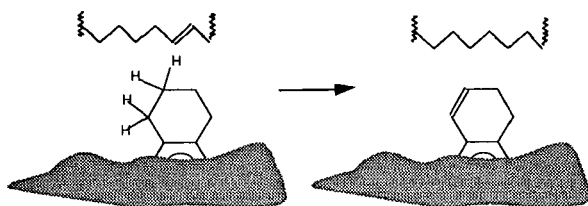
Also presented in the figures are the predicted distributions based on eq (1), starting with the D<sub>0</sub>-isomer, and adjusted to peak respectively at D<sub>3</sub> and D<sub>2</sub>. Clearly in 1a the observed distribution is far broader than the calculated one; there is both far more D<sub>0</sub> and significant isotope substitution beyond D<sub>8</sub> in the recovered product than predicted in the simple statistical model. A similar lack of fit is observed for the other *n*-alkanes recovered in the work.

The match in 1b on the other hand is very good. The added olefin obviously behaves differently from thermally generated, kerogen-derived alkane precursors. It must be quickly reduced to the protio alkane, which then exchanges as in eq (1).

Accordingly, to explain the generation of alkane from kerogen, the thermal generation of olefin must be included in our considerations, as shown in the scheme in (2). The scheme includes separate pyrolysis, reduction, and exchange steps, and a branching step for dry pyrolysis to be discussed below. Since the olefin reduction is rapid,  $r_{rd} \gg r_{py}$ , the rate of alkane production is essentially the pyrolysis rate. We presume the reduction step to proceed necessarily by way of reaction with the nonexchangeable protium in the organic



phase, i.e.



while exchange must take place on the mineral surfaces which have been equilibrated with  $D_2O$ .

We can next consider a selection of scenarios in which the ratios  $r_{py}/r_{ex}$  are varied over a range of values (Figure 2). The *n*-heptadecane profile is also shown in the figures. They show that for a fixed exchange rate a relatively high alkane production rate provides a distribution shown in 2a like that in 1a except in this case the peak is at  $D_6$ . Reducing the ratio by an order of magnitude rolls the peak down to lower D-values, and provides a satisfactory fit to the observed profile as shown in 2b. Decreasing the ratio still further in 2c yields a profile favoring the low-D side, as would be expected as the conditions shift toward what is effectively a large reservoir and a steady-state supply of precursor.

The match in 2b supports the sense of the scheme in eq (2) that alkane precursor supply is not instantaneous, but with a rate comparable to that for exchange. Thus for the Hoering work,  $r_{rd} \gg r_{py} = r_{ex}$ . A key aspect of this exercise is the comparison of figures 1b and 2b, for which the ratio of exchange rates necessary for the observed fits,  $r(2b)_{ex}/r(1b)_{ex}$ , is about 3. This result is in line with the difference in the H/D ratios for the olefin-added and kerogen-derived alkanes in Table 1. Since the exchange is mineral surface promoted, these data reflect an extensive association of the kerogen with the mineral surface in the source rock, and extensive chemistry specific to the interface.

#### Autoradiological Probe of the Mineral/Organic Boundary

It is recognized that silica surfaces bind hydrocarbons in what must be donor-acceptor complexes (Iler, 1979). Similarly, oxygen-containing compounds including benzoates, phthalates, salicylates, phenols, and catechols complex with aluminum oxides and hydrox-

ides (Davis and Hem, 1989). However little is known about the interactions at the phase boundary and the nature of the bridging structures.

In recent studies directed at the formation and durability of asphalt-aggregate bonds in highways we have developed some relevant data using tritium-tagged organics and autoradiographic techniques as sketched in Figure 3 (Ross, et al., 1991). Clean surfaces of several aggregate samples were exposed to very dilute solutions of the compounds 4-HO<sub>2</sub>C-C<sub>6</sub>H<sub>5</sub>(CHT)<sub>2</sub>(CH<sub>2</sub>)<sub>10</sub>CH<sub>3</sub> (I) and C<sub>6</sub>H<sub>5</sub>(CHT)<sub>2</sub>(CH<sub>2</sub>)<sub>10</sub>CH<sub>3</sub> (II) in refluxing toluene (111°C/~30 min).<sup>\*</sup> The samples were then extracted with toluene in a Soxhlet (20 hr), and the flat surface was mated to fast photographic film. Following 8-day exposures the samples were extracted with water in a Soxhlet (100°C/2 hr), and photographed again.

The results for a rock sample containing primarily silica and K-feldspar (potassium aluminosilicate) treated with the carboxylic acid (I) are presented in Figure 4. The images in 4a and 4b show the results following the toluene and water extractions, respectively, and both show remaining organic material in a mosaic of distinct bonding and nonbonding zones. 4b is less intense than 4a, a significant result demonstrating the removal of some but not all of the material.

This result cannot be reconciled with simple acid-base association between (I) and the surface since such complexing would be fully destroyed by water. It is recognized that benzene yields a carbonaceous film on clean platinum surfaces at around 100°C (Davis and Somorjai, 1980), and aluminosilicates engage in similar activity (Somorjai, 1991). However the phenomenon has received little study, and little is known about the nature of the films nor of their bonding to the mineral surface. We surmise that the tritium-containing substances bound to the mineral surface are residues from surface promoted decomposition, and are very strongly bound to the surface.

The character of the sites associated with the films is revealed in SEM/EDAX studies of the same rock surface presented in Figure 5. 5a is an enlarged portion of 4b (top, left of center), and 5b is the SEM image of that region at about 50 x magnification. K and Si maps of the same region are shown in Figures 5c and 5d, respectively; Ca, Al, and Fe maps were also prepared but are not shown. The figure shows the Si distribution to be uniform over the region, as are the Ca and Fe distributions although they show a lower density of spots. The K and Al maps, however, shows distinct patterns of K-rich and -poor regions, which are, respectively, feldspar, a potassium aluminosilicate, and silica.

Comparison of the image in Figure 5a and the K map in Figure 5c shows an unmistakable similarity in patterns. This match demonstrates a preferential reactivity of, and bonding to, the feldspar regions of the rock. Examination of the SEM image of the surface in 5b shows a faint pattern also matching the K map. Such patterns are not visible in aggregate that has not been treated, and reflect the deposition of the film in the active regions.

Subsequently the unsubstituted arene II was studied with aggregate samples that were virtually fully silica, and provided faint but well defined images faithful to the exposed silica surface following the toluene-stripping (not shown). Water-stripping in this case eliminated all trace of the signal. There is little doubt that the silica surfaces in the studies with I show some signal; however it is difficult to be observed because of the much stronger response in the feldspar regions. This result, a carbonaceous film surviving 20 hr of toluene extraction derived from an organic compound with not polar functionality on a relatively unreactive surface, demonstrates the likely ubiquity of these films, and their possible significance in source rock and the maturation process.

<sup>\*</sup> The solutions also contained asphalt, an aspect of the work not important to the discussion here.

## CONCLUSIONS

The action of water at the organic-mineral interface is apparent from the diminishing signal in Figures 4a and 4b. The water in some manner strips some of the organic material from the surface. It is conceivable that the stripping involves hydrolysis of the mineral phase supporting the organic film rather than action at the bonds bridging the two phases. Whatever the specific mode of action, the process should be important in hydrous pyrolysis in separating the two phases.

This activity goes hand in hand with the moderation of the acidity of mineral sites by water, as recognized by Tannenbaum and Kaplan (1985). Acidic sites on clay surfaces have been invoked as a significant feature of maturation (Alexander, et al., 1982, 1984), and water must therefore be significant to the degree and direction of that chemistry. We have utilized these views in eq (2), suggesting that in the absence of water the high surface acidity irreversibly reincorporates the pyrolytic products into the organic phase as char.

Thus since aromatization is a major driving force during maturation (Hayatsu et al., 1987), and therefore a source of hydrogen (or reduction potential), we can envision a system which in the absence of water the organic phase remains associated with the mineral phase, and thermolytically releases hydrogen and relatively small quantities of olefin. The major product is an H-poor char on the surface. In contrast when water is present, the phases are separated, the moderated surface acidity reduces char formation, and the olefins are available for reduction to alkanes. The alkanes then engage in hydrogen exchange with other appropriate sites on the mineral surface before escaping into the aqueous medium, which at near critical temperatures is a good alkane solvent (Skripka, 1979).

## ACKNOWLEDGEMENT

It is a pleasure to acknowledge very useful discussions of hydrous pyrolysis with my colleagues Dr. Donald McMillen and Dr. Ripudaman Malhotra. Dr. McMillen was helpful in clarifying the important issue of a mixed ionic/free radical sequence for protium/deuterium exchange, and Dr. Malhotra emphasized the point that slow kerogen thermolysis could be significant in the product isomer patterns.

## REFERENCES

- Alexander, R., Kagi, R. I., and Larcher, A. V., 1982. *Geochemica et Cosmochimica Acta*, **46**, 219-222.
- Alexander, R., Kagi, R. I., and Larcher, A. V., 1984. *Organic Geochemistry*, **6**, 755-760.
- Comer, P. A., McEvoy, J., Giger, W., and Douglas, A. G., 1986. *Organic Geochemistry*, **2**, 171-182.
- Commins, B. T., 1969. *Atm. Env.*, **3**, 565-572.
- Davis, J. and Hem, J., 1989. *The Environmental Chemistry of Aluminum*, G. Sposito, Ed., CRC Press, Inc., Boca Raton, FL, pp 186-218.
- Davis, S., and Somorjai, G., 1980. *J. Catalysis*, **65**, 78-83.
- Hayatsu, R., Botto, R. E., Scott, R. G., McBeth, R. L., and Winans, R. E., 1987. *Organic Geochemistry*, **11**, 245-250.
- Hoering, T. C., 1984. *Org. Geochem.*, **5**, 267-278.

- Iler, R., 1979. *The Chemistry of Silica*. John Wiley and Sons, New York, pp. 652-653 and 656-657.
- Lewan, M. D., Winters, J. C., and McDonald, J. H., 1979. *Science*, **203**, 897-899.
- Lewan, M. D., Winters, J. C., and Williams, J. A., 1981. *Adv. in Organic Geochemistry 1979*, M. Bjorøy et al., eds., John Wiley and Sons, Ltd., Chichester, p. 524-533
- Monthieux, M., Landais, P., and Monin, J.-C., 1985. *Organic Geochemistry*, **8**, 275-292.
- Moore, J., and Pearson, R., 1981. *Kinetics and Mechanism*, Third Edition, John Wiley and Sons, New York, 318-324.
- Ross, D. S., Loo, B., and Mirsalis, J., 1991. Fundamentals of the Asphalt-Aggregate Bond, Report prepared for the Strategic Highway Research Program, Contract No. SHRP-87-AIIR-11.
- Ross, D. S., 1992. *Organic Geochemistry*, **18**, 79-81.
- Simoneit, B.R.T., 1985. *Can. J. Earth Sci.*, **22**, 1919-1929.
- Simoneit, B.R.T., Grimalt, J. O., Hayes, J. M. and Hartman, H., 1987. *Geochim. Cosmochim. Acta*, **51**, 879-894.
- Skripka, V. G., 1979. *Chemistry and Technology of Fuels and Oils*, **15**, 88-90.
- Somorjai, G., 1991. Personal communication.
- Tannenbaum, E. and Kaplan, I. R., 1985. *Nature*, **317**, 708-709.

Table I

D-Introduction into Recovered Alkane<sup>a</sup>

	From added <i>n</i> -octadecane	<i>n</i> -Octadecane from added octadecene	Kerogen-derived <i>n</i> -C <sub>17</sub> - C <sub>29</sub>
%-D-containing <sup>b</sup>	28	91	94-96
D/H	0.02	0.09	>0.20 <sup>c</sup>

a. From Hoering, 1984

b. Fraction of recovered alkane with at least one deuterium atom.

c. The D-quantities were not presented beyond D<sub>14</sub>, but the exchange pattern suggests significant contribution by more highly exchanged isomers. The D/H value is thus a lower limit.

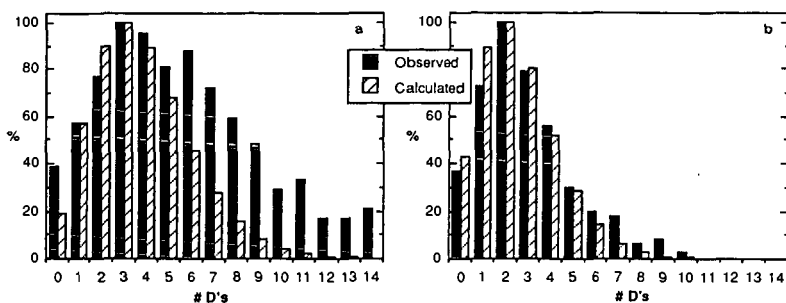


Figure 1. a) D-distribution for kerogen-derived heptadecane and calculated profile.  
b) D-distribution for octadecene-derived octadecane and calculated profile. In both cases the calculation is for simple exchange via eq. 1.

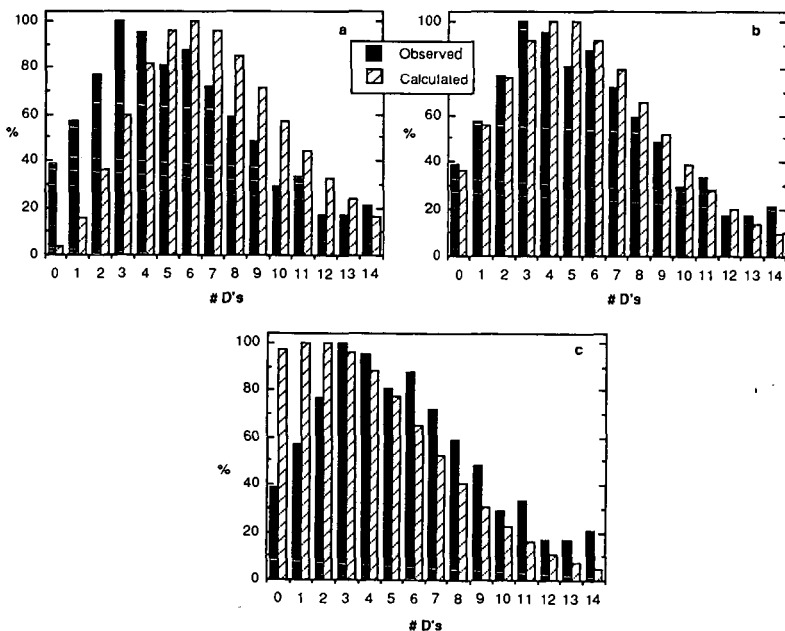
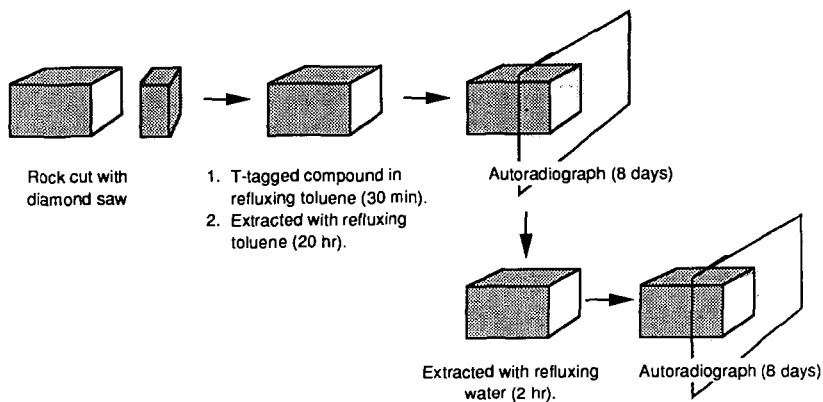


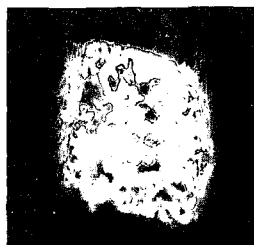
Figure 2. D-profile for kerogen-derived heptadecane and calculated profiles via eq. 2.  
a)  $r_{py}/r_{ex} = 4.60$  b)  $r_{py}/r_{ex} = 0.46$  c)  $r_{py}/r_{ex} = 4.6 \times 10^{-2}$



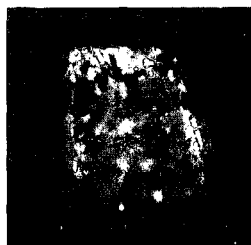


CAM-2847-2

Figure 3. Sequence for autoradiographic study.



(a) AR image after toluene-stripping



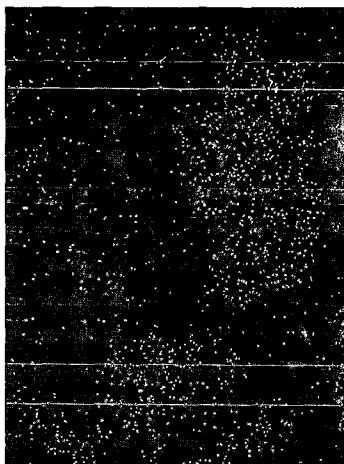
(b) AR image after water-stripping

CPM-2847-1

Figure 4. Autoradiograph images following treatment with  $\text{HO}_2\text{C-Ar(CHO)}_2(\text{CH}_2)_{10}\text{CH}_3$ .



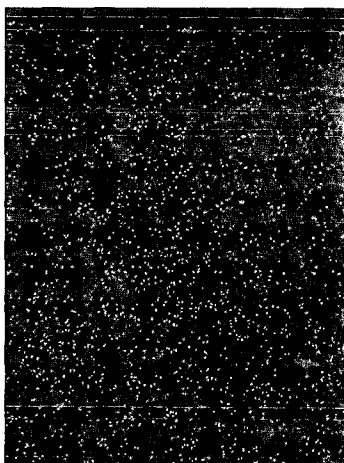
(a) AR Image



(c) K Map



(b) SEM Image



(d) Si Map

RP-8674-8A

Figure 5. SEM/EDAX studies of test piece with carboxylic acid.